Channel Estimation and Physical Layer Security in Optical MIMO-OFDM based LED Index Modulation

F. Batuhan Okumus, Erdal Panayirci, Mohammad Ali Khalighi

Channel Estimation and Physical Layer Security in Optical MIMO-OFDM based LED Index Modulation

F. Batuhan Okumus[1], Erdal Panayirci[1] and Mohammad Ali Khalighi[2]
[1]*Electrical and Electronics Engineering, Kadir Has University, Istanbul, Turkey*,
[2]*Aix-Marseille University, CNRS, Centrale Marseille, Institut Fresnel, Marseille, France*
furkan.okumus@khas.edu.tr, eepanay@khas.edu.tr, Ali.Khalighi@fresnel.fr

***Abstract*—In this paper, we propose a new and low-complexity channel estimation algorithm for the generalized LED index modulation (GLIM), recently proposed for visible-light communication systems based on multi-input multi-output (MIMO) and orthogonal frequency-division multiplexing (OFDM). For this scheme, denoted by GLIM-OFDM, we investigate the bit-error rate (BER), the mean-square error (MSE) of channel estimation, as well as the Cramer-Rao bound on the latter. Furthermore, we present a novel physical layer security (PLS) technique for the GLIM-OFDM scheme using precoding at the transmitter assuming it has the channel state information (CSI) between the LEDs and a legitimate user, but no knowledge of the CSI corresponding to eavesdroppers. The efficiency of the proposed PLS technique is demonstrated through numerical results.**

***Index Terms*—Visible light communication(VLC), Orthogonal frequency division multiplexing(OFDM), Generalized LED index modulation OFDM(GLIM-OFDM), Channel Estimation (CE), Physical Layer Security (PLS)**

I. Introduction

Future 6G networks are expected to provide extremely high capacity and superior coverage in diverse application scenarios. To address the radio-frequency (RF) congestion, optical wireless communications (OWC) and, more specifically, visible-light communications (VLC) are being considered as part of such networks as complementary technologies to RF transmission. VLC is particularly promising in indoor scenarios thanks to its advantages of wide license-free spectrum, low cost, energy efficiency, and inherent security [1].

VLC uses light-emitting diodes (LED) at the transmitter to carry information by light intensity. The data is recovered at the receiver typically using a photodetector; this approach is known as intensity modulation and direct detection (IM/DD). To address the limited bandwidth of the LEDs, as well as the channel frequency selectivity (in particular in the case of blocked line-of-sight, LOS), Orthogonal frequency division multiplexing (OFDM) and its modified versions for intensity modulation/direct detection (IM/DD) systems in VLC have attracted significant attention due to frequency-selective behavior of the VLC channels for moderate and high data rates and the capability of easily achieving bit and power loading [2]. Given the requirement of IM/DD systems to use real and positive signal levels (for intensity modulation), different optical OFDM techniques have been proposed in the literature so far. The simplest approach, called DC-biased optical OFDM (DCO-OFDM), uses a DC bias after the inverse fast-Fourier-transform (IFFT) operation and lower signal clipping [3]. Also, the asymmetrically-clipped optical OFDM (ACO-OFDM) exploits the FFT's anti-symmetric feature [4], while having a spectral efficiency penalty of factor 2, compared to DCO-OFDM [5]. Unipolar optical OFDM (U-OFDM) is another alternative popular approach proposed in [6], as well as it combination with ACO-OFDM to improve its spectral efficiency, as proposed in [7], [8]. On the other hand, several techniques have been proposed to manage multiple-user transmission [**?**] , including based on multi-input multi-output (MIMO) architectures On the other hand. For this latter, spatial modulation (SM), which is the most common form of index modulation was proposed in [11], [12] for VLC systems. Also, a novel generalized light emitting diode (LED) index modulation method is proposed for MIMO OFDM-based VLC systems that avoids the typical spectrum efficiency losses incurred by time-and frequency-domain shaping in OFDM signals. Nevertheless, only few studies have investigated the impact of channel estimation errors related to VLC systems as well as to GLIM-OFDM [13], [14]. In this paper, an efficient and low-complexity channel estimation technique is proposed for a 4×4 MIMO-VLC system using the so-called generalized optical OFDM scheme, proposed in [15]. We investigate the performance of the proposed method based on the link bit-error rate (BER) and the mean-square-error (MSE) of the channel estimator for different modulation orders. The Cramer-Rao lower bound (CRLB) on the estimation errors is also derived and compared with the MSE.

Meanwhile, it is evident that physical layer security (PLS) will play a vital role in enhancing cyber-security in 6G wireless networks. Particularly, it will imply a low latency and a low computational complexity, compared with the conventional cryptography techniques, e.g., based on using secret and public key encryption methods. Moreover, in the latter approach the physical layer exposes significant vulnerabilities due to the broadcast nature of the wireless channel, and additional security precautions need to be adopted in this layer. As a result, PLS techniques become of critical importance, in particular for machine-type communications. There have been significant developments recently in the design of PLS methods for VLC , for instance, by employing some MIMO-based index-modulation techniques with precoding [19], [20], [21], [22], [23]. Here, we propose a novel precoding-based PLS technique for the GLIM-OFDM transmission scheme. Based on the CSI of the legitimate user at the transmitter, the precoding matrix coefficients are constructed through some optimization techniques so that the confidential message is perceived by the legitimate user clearly, while resulting in a substantial degradation of the eavesdropper's BER performance.

II. Optical GLIM OFDM in Frequency-Flat MIMO Channels

The GLIM-OFDM transceiver block diagram for frequency-flat MIMO channels is given in Fig. 1. Information bits $N \log_2(M)$

[1]This research has been supported in part by the Scientific and Technical Research Council of Turkey (TUBITAK) under the 1003-Priority Areas R&D Projects Support Program No. 218E034. It is based upon work from COST Action NEWFOCUS, supported by COST (European Cooperation in Science and Technology).

carrying the vector $\mathbf{u}$ are applied to the GLIM-OFDM transmitter for transmission of each OFDM block, where N is the number of OFDM subcarriers and M is the size of M-level quadrature amplitude modulation (M-QAM) signals used in transmission. The operation of DCO-OFDM, ACO-OFDM and non-DC-biased OFDM (NDC-OFDM) optical communication systems relies on Hermitian symmetry to generate real-time signals after the IFFT process. In the GLIM-OFDM, the OFDM modulator directly processes the complex frequency domain OFDM frame $\mathbf{x}_F$ without requiring Hermitian symmetry. The resulting time-domain OFDM frame $\mathbf{x}_T$=[x_1 … x_N]^T is composed of complex-valued and bipolar (positive and negative-valued) elements; therefore, it cannot be transmitted via a VLC channel. To solve this problem, a new LED index modulation-based MIMO transmission technique has been developed. After parallel to serial (P/S) conversion, using a technique similar to [16], for each time-domain OFDM signal x_k, where $k = 0, 1,\ldots, N-1$, first the real and imaginary parts of the complex signal x_k are separated where x_k=$x_{k,R} + jx_{k,I}$. The resulting real but bipolar signals $x_{k,R}$ and $x_{k,I}$ are then processed by positive-negative (+/-) separators to yield the following positive real-valued signals:

$$x_{k,R}^{+} = \begin{cases} x_{k,R}, & \text{if, } x_{k,R} > 0 \\ 0, & \text{if, } x_{k,R} < 0 \end{cases} \quad x_{k,R}^{-} = \begin{cases} 0, & \text{if, } x_{k,R} > 0 \\ -x_{k,R}, & \text{if, } x_{k,R} < 0 \end{cases}$$

$$x_{k,I}^{+} = \begin{cases} x_{k,I}, & \text{if, } x_{k,I} > 0 \\ 0, & \text{if, } x_{k,I} < 0 \end{cases} \quad x_{k,I}^{-} = \begin{cases} 0, & \text{if, } x_{k,I} > 0 \\ -x_{k,I}, & \text{if, } x_{k,I} < 0 \end{cases}$$

These signals are transmitted simultaneously from an $n_R \times n_T$ MIMO VLC system, where n_R and n_T indicate the number of the receiver (Rx) and transmitter (Tx) units, respectively. As can be seen from Figure 1, the LEDs transmit the absolute values of the $x_{k,R}$ and $x_{k,I}$ signals and are thus positive real numbers. Also, unlike other optical communication systems, GLIM-OFDM completely eliminates the Hermitian symmetry at the input of the IFFT and the loss of spectral efficiency caused by Hermitian symmetry. As a result, the spectral efficiency of the GLIM OFDM system is $\log_2(M)$ [bit/s/Hz], achieving a spectral efficiency up to twice that of conventional systems. Positive and real-valued OFDM time samples $x_{k,R}^{+}$, $x_{k,R}^{-}$, $x_{k,I}^{+}$ and $x_{k,I}^{-}$ where $k = 0, 1, \ldots, N-1$ are transmitted over a 4×4 optical MIMO channel which is represented by H as,

$$\mathbf{y} = \mathbf{H}\mathbf{x} + \mathbf{n} \tag{1}$$

where $\mathbf{y} = [y_{k,I} \ldots y_{k,n_R}]^T \in \mathbb{R}^{n_R \times 1}$ is the vector of received signals that contains the electrical signals obtained from PDs at the Rx units. In Eq.1, $\mathbf{n} \in \mathbb{R}^{n_R \times 1}$ is the vector of real-value AWGN that models shot and thermal noises. The elements have a probability distribution $N(0,\sigma_w^2)$ and are added to received signals in the electrical domain. The transmitted signal vector $\mathbf{x} \in \mathbb{R}^{4\times 1}$ is generated for GLIM-OFDM as:

$$\mathbf{x} = [x_{k,R}^{+} x_{k,R}^{-} x_{k,I}^{+} x_{k,I}^{-}]^T. \tag{2}$$

Over a 4×4 optik MIMO channel which is shown as $\mathbf{H} = [h_{r,t}]$, $h_{r,t}$ represents the channel gain of the optical wireless channel formed between the t^{th} LED at the transmitter and the r^{th} PD at the receiver. In this study, the SNR is defined as the average SNR at the receiver:

$$SNR_{Rx} = \frac{P_{Rx}^{elec}}{\sigma_n^2} \tag{3}$$

where P_{Rx}^{elec} is the average electrical power reaching the receiver and σ_n^2 is the noise power at the receiver.

III. Channel Estimation in GLIM OFDM Systems

The block diagram shown in Fig. 1 represents a GLIM OFDM system with precoder and channel estimation. As a first step, we need to estimate the channel at the receiver side and send it the channel state information (CSI) back to the precoder at the transmitter side of the system by a different uplink infrared channel. Therefore, the correctness of the estimation of the channels is vital for the correct operation of the system. In this study, we propose a channel estimation algorithm with a low computational complexity that ensures a BER for the system, almost the same as the scenario when the channel is already known. It also provides an MSE performance that has nearly reached the CRLB.

In GLIM OFDM, the positive and real-valued time-domain signal vector of the time-domain components arriving at the receiver's FFT input can be expressed as:

$$\mathbf{y}_k = \mathbf{H}\mathbf{x}_k + n_k \tag{4}$$

where the $\mathbf{x}_k \in \mathcal{R}^{4\times 1}$ vector represents the time-domain sample vectors generated at the IFFT output at the transmitter side of the system for each $k = 0, 1, \cdots, N-1$, and $\mathbf{n}_k \in \mathcal{R}^{4\times 1}$ represents the additive white Gaussian noise vector whose components are statistically independent. To estimate the channel matrix within each given time frame, the signal vectors $\mathbf{X} = [\mathbf{x}_0, \mathbf{x}_1, \cdots, \mathbf{x}_{N-1}]$ generated from the pilot symbols will be assumed to be known at the receiver. In this case, the receiver signal can be expressed as:

$$\mathbf{Y} = \mathbf{H}\mathbf{X} + \mathbf{N}, \tag{5}$$

and, $\mathbf{Y} = [\mathbf{Y}_0, \mathbf{Y}_1, \cdots, \mathbf{Y}_{N-1}] \in R^{4\times N}$ and $N = [\mathbf{n}_0, \mathbf{n}_1, \cdots, \mathbf{n}_{N-1}] \in R^{4\times N}$ Using classical matrix relations, the matrix $\mathbf{Y}$ can be expressed as a $4N$ dimensional vector as follows:

$$\tilde{\mathbf{y}} = \mathbf{Q}\mathbf{h} + \tilde{\mathbf{n}} \tag{6}$$

where $\tilde{\mathbf{y}} = \text{vec}(Y)$, $\tilde{\mathbf{n}} = \text{vec}(N)$ and $\mathbf{Q} = \mathbf{X}^T \otimes \mathbf{I}_r$ and $\otimes$ shows the Kronocker product. Using the linear observation equation in 6, the linear minimum mean-square estimation (LMMSE) for the unknown channel $\mathbf{h}$ is obtained as follows:

$$\widehat{\mathbf{h}}_{\text{LMMSE}} = \mathbf{Q}^T \left(\mathbf{Q}\mathbf{Q}^T + (1/\rho)\mathbf{I}_r \right) \tilde{\mathbf{y}} \tag{7}$$

where $\rho = I/\sigma_n^2$ ve $I = 1/\sqrt{2\pi}$ is equal to the square of the statistical mean of the sample values $|x_{k,R}|$ and $|x_{k,I}|$ with a folded-Gaussian probability distribution. If the error vector in the channel estimation calculated with this relationship is $\mathbf{e} = \widehat{\mathbf{h}}_{LMMSE} - \mathbf{h}$, then MSE is defined as:

$$\text{MSE} = \mathbb{E}\left\{ (\widehat{\mathbf{h}}_{\text{LMMSE}} - \mathbf{h})^T (\widehat{\mathbf{h}}_{\text{LMMSE}} - \mathbf{h}) \right\}.$$

Using this definition, the mean square error in the channel estimation considered is obtained as follows:

$$\text{MSE} = \frac{1}{\sqrt{2\pi}} \left(1 - \mathbf{Q}^T \left(\mathbf{Q}\mathbf{Q}^T + (1/\rho)\mathbf{I} \right) \mathbf{Q} \right).$$

A. Cramer-Rao Lower Bound in Channel Estimation

The lower limit of the mean error in the obtained channel estimation is determined by the CRLB and this limit is calculated as following:

$$\text{MSE} = \mathbb{E}\{ (\hat{\mathbf{h}} - \mathbf{h})^T (\hat{\mathbf{h}} - \mathbf{h}) \geq \mathbf{I}^{-1}(\mathbf{h}) \}. \tag{8}$$

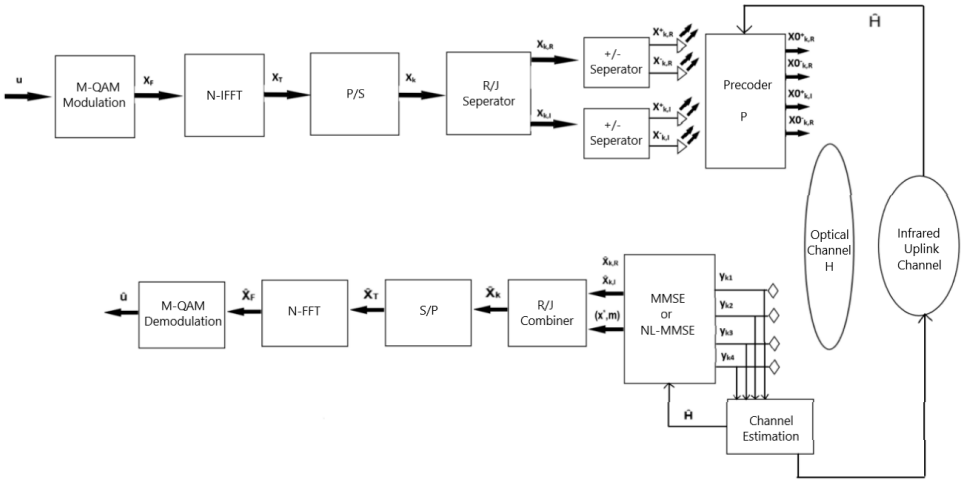

Fig. 1. Block Diagram of the GLIM-OFDM for a 4x4 MIMO-VLC system

where $\hat{\mathbf{h}} \triangleq \widehat{\mathbf{h}}_{\text{LMMSE}}$ and $\mathbf{I^{-1}}(\mathbf{h})$ is named *Cramer-Rao* lower-bound. It is calculated from:

$$\mathbf{I}(\mathbf{h}) = E\left\{ \frac{\partial^2 \ln p(\tilde{\mathbf{y}}; \mathbf{h})}{\partial \mathbf{h}^2} \right\}. \tag{9}$$

In this relation, $p(\tilde{\mathbf{y}}; \mathbf{h})$ shows the probability density function of the signal arriving at the receiver modeled as $\mathbf{Qh} + \mathbf{w}$ and it can be expressed as:

$$p(\tilde{\mathbf{y}}; \mathbf{h} \sim \exp\left\{ \frac{1}{\sigma_n^2} (\tilde{\mathbf{y}} - \mathbf{Qh})^T (\tilde{\mathbf{y}} - \mathbf{Qh}) \right\}$$

By taking the 2nd partial derivative of $p(\tilde{\mathbf{y}}; \mathbf{h})$ as in Eq. 9, the following expression is obtained for $\mathbf{I}$:

$$\mathbf{I}(\mathbf{h}) = \frac{1}{\sigma_w^2} \mathbf{Q}^T \mathbf{Q}.$$

Finally, the Cramer-Rao lower bound for the channel estimation obtained with the help of this expression is found as follows:

$$\text{MSE} \geq \sigma_w^2 \text{trace}(\left(\mathbf{Q}^T \mathbf{Q}\right)^{-1}). \tag{10}$$

IV. Trasmitter Precoded Aided PLS in GLIM OFDM

With the aid of the legitimate user's (Bob) channel state information at the transmitter (CSIT), the bit error rate (BER) performance of Bob is minimized over the provided co-channel interference-free and low complexity transmission between the source and Bob. On the other hand, the BER of the eavesdropper (Eve) is degraded significantly. To achieve the above objective, the precoding matrix $\mathbf{P}$ has to ansure that no energy leakage among the receiving PDs. For this purpose, the zero-forcing (ZF) precoding or the minimum mean square error (MMSE) precoding may be used. We adopt the ZF precoding in this work whose precoding matrix $\mathbf{P}$ is constructed from the pseudo-inverse of the Bob's channel $\mathbf{H}_B$ as

$$\mathbf{P} = \beta \left(\mathbf{H}_B^T \mathbf{H}_B \right)^{-1} \mathbf{H}_B^T \tag{11}$$

where $\beta = \sqrt{N_r / \text{trace}(\mathbf{P}^T \mathbf{P})}$ is a normalizing factor. It can eliminate the co-channel interference among the receiving PDs completely by preprocessing the source signal $\mathbf{x} = [x_{k,R}^+, x_{k,R}^-, x_{k,I}^+, x_{k,I}^-]^T \in \mathbb{R}^{n_R \times 1}$ before its transmission. Consequently, a low-complexity signal stream estimation of $\mathbf{x}$ becomes possible at the receiver of the legitimate user(Bob), independent of the channel parameters. However, since the channel $\mathbf{H}_E$ between the source and an eavesdropper (Eve) is different from Bob's channel, the precoded source signal will be received by Eve with a jamming signal generated as a result of the precoding mismatch with Eve's channel. After transmit precoding, the time-domain, positive and real-valued OFDM sample vectors $\mathbf{x}$ are converted into an optical signal $\mathbf{u}$, which can be written as

$$\mathbf{u} = \mathbf{Px}. \tag{12}$$

where the signals emitted by the LEDs are indicated as the elements of $\mathbf{u}$. According to the (1), for a given OFDM signal, only two out of four elements are non-zero, i.e., two LEDs remain inactive (turned off). In this way, the proposed scheme utilizes the index modulation concept for the active LED indices to transmit the complex OFDM signals. Finally, the signal observed at the N_r PDs of Bob (B) and Eve (E) after propagation through their respective channels may be written as

$$\mathbf{y}_{\text{B}} = \beta \mathbf{x} + \mathbf{n}_{\text{B}}, \tag{13}$$

$$\mathbf{y}_{\text{E}} = \beta \mathbf{G} \mathbf{x} + \mathbf{n}_{\text{E}}, \tag{14}$$

where $\mathbf{G} \triangleq \mathbf{H}_{\text{E}} \left(\mathbf{H}_{\text{B}}^T \mathbf{H}_{\text{B}} + \epsilon \mathbf{I}_{N_r} \right)^{-1} \mathbf{H}_{\text{B}}^T$. where, $\mathbf{y}_B, \mathbf{y}_E \in \mathbb{R}^{n_R \times 1}$ are the vectors of received signals that contains the electrical signals obtained from PDs of the Bob's and Eve's Rx units. In Eqs 13 and 14, $\mathbf{n}_B, \mathbf{n}_E \in \mathbb{R}^{n_R \times 1}$ are the vectors of real-valued additive white Gaussian noise (AWGN) samples, that models the shot noise and thermal noise in the Bob's and Eve's channels, with variances, σ_{B}^2 and σ_{E}^2, respectively.

A straightforward solution to the estimation problem formulated in (13) and (14) is the use of the zero-forcing (ZF) equalizer, which yields an estimate of $\mathbf{x}$ simply as

$$\hat{\mathbf{x}}_{ZF} = \begin{cases} \frac{1}{\beta} \mathbf{y}_B, & \text{for BOB's transmisson} \\ \frac{1}{\beta} \mathbf{G}^{-1} \mathbf{y}_E & \text{for EVE's transmisson.} \end{cases} \tag{15}$$

After this operation, the receiver can determine the indices of the active LEDs and corresponding signals by selecting the higher magnitude signals from $\hat{\mathbf{x}}_{ZF}$. Finally, classical OFDM processing steps such as serial-to-parallel (S/P) conversion, FFT,and M-ary demodulation are applied to obtain to detect the transmitted information.

V. Computer Simulations

In this study, the Bob's and Eve's channels are created with Zemax software between the illuminators (LED), placed on the ceiling in a room of a square prism (5m $\times$5 m $\times$3 m). The photodetectors (PD)of Bob and Eve are placed at the corners of tables (0.1m $\times$0.1 m $\times$0.8 m). The field-of-view (FOV) semi-angle and area of the PD are 70°and 1 cm2, respectively. Luminaries and PDs are assumed to be facing vertically downward to the floor and upward to the ceiling, respectively. The half-power and half-angle of the LEDs and the areas of the PDs are assumed to ben$\Phi_{1/2} = 2 = 60^o$; $\Psi_{1/2} = 70^0$; $A_{PD} = 1$ cm2.

A. Simulation Results for Channel Estimation

For channel estimation, it is necessary to add pilot symbols. For this purpose, different subcarriers in the frequency domain of OFDM are generally reserved for carrying pilot symbols. However, in the VLC-based OFDM system proposed in this paper, all sub-carriers of the first OFDM symbol in a given frame of M OFDM symbols are allocated to pilot symbols using the same modulation format as the data symbols. Consequently, data transmission occurs from all sub-carriers of other OFDM signals in the frame. The (x, y, z) coordinates of the LEDs and PDs in m, as well as the corresponding channel gains for Bob's channel is generated by the Zemax© software are shown below:

LED coordinates: [(-1.3 -0.7 3); (-1.3 1.3 3); (0.7 1.3 3) ; (0.7 -0.7 3)],

PD coordinates: [(-0.05 -0.05 0.8); (-0.05 0.05 0.8); (0.05 -0.05 0.8); (0.05 0.05 0.8)],

$$\mathbf{H_B} = 1.0e-05 * \begin{bmatrix} 0.2185 & 0.0444 & 0.0213 & 0.0557 \\ 0.2026 & 0.0411 & 0.0202 & 0.0536 \\ 0.2294 & 0.0453 & 0.0223 & 0.0599 \\ 0.2124 & 0.0420 & 0.0211 & 0.0576 \end{bmatrix}$$

.

Based on this configuration, the Bob's channel is estimated using the estimation algorithm described in the previous section, and the bit error performance is determined at the receiver using the estimated channel state information (CSI) within each OFDM frame. In Figure 2, the MSE error performances of the channel estimation algorithm for 4QAM, 8QAM and 16QAM constellations are obtained as functions of the signal-to-noise ratio with the number of OFDM subcarriers $N = 128$ in the system. It is concluded from Fig. 2 that the proposed channel estimation algorithm works very effectively with minimal computational complexity and is almost entirely independent of the different levels of modulation techniques employed. It is also seen that the MSE performance nearly reaches the Cramer-Rao lower bound.

In Figure 3, the BER performance of the data detection process is examined for the 4QAM, 8QAM and 16QAM modulations as a function of the signal-to-noise ratio, employing the estimated CSI. As can be clearly seen from this figure, the BER performance level of the system that can be reached under the presence of channel estimation errors is very closed to those obtained with perfect CSI at each modulation level.

B. Simulation Results for PLS

This section presents the simulation results for the PLS performance of the proposed GLIM OFDM indoor LiFi system. We consider three different user scenarios as shown in Fig. 4. The symbols S_1, S_2, S_3, S_4 represent the LEDs transmitting the four components of the OFDM complex-valued time samples. The white and black

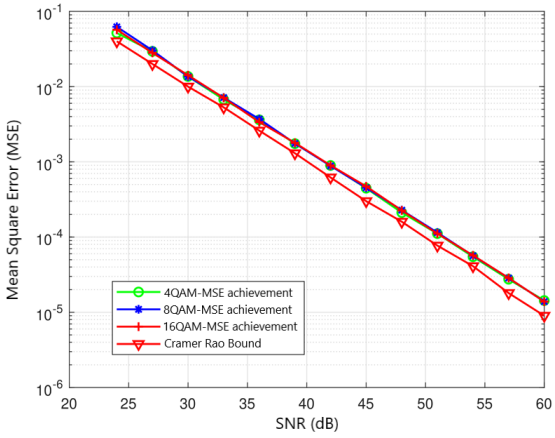

Fig. 2. Channel Estimation MSE Performance and Cramer-Rao Lower Bound

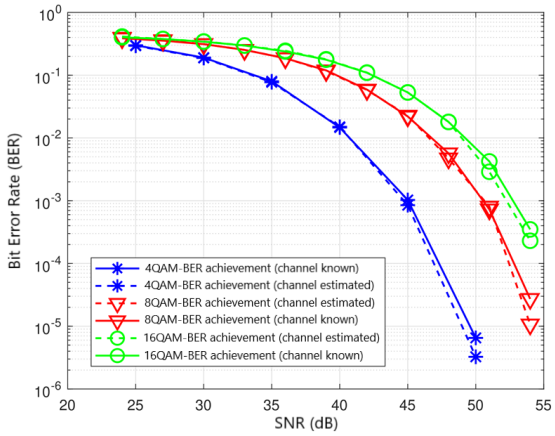

Fig. 3. GLIM OFDM BER Performance Under Channel Estimation Error

figures of the bottom one represent Bob and Eve, respectively. These scenarios are different based on the relative positions as compared to the room's middle line (dashed line). The BER performance of the legitimate user (Bob) and eavesdropper (Eve) is investigated through the computer simulations based on the channel matrices $\mathbf{H}_B$ and $\mathbf{H}_E$ obtained by Zemax© software. As seen from Fig. 5, Bob's BER performance outperforms the performance of Eve substantially. While the BER of Bob reaches 10^{-5} at SNR values between 20-30 dB, Eve's BER is not below 3×10^{-1} in a similar SNR range.

VI. Conclusions

In this paper, a channel estimation algorithm with low computational complexity has been developed in a generalized index modulation OFDM-based PLS system. Within the scope of the paper, a new pilot-aided channel estimation technique is proposed with low computational complexity for efficient estimation of the optical channel of a GLIM-OFDM system. The Cramer-Rao lower bound, a measure of the MSE performance of the channel estimation algorithm, is obtained analytically. From the computer simulations, it was concluded that the MSE performance of the proposed channel estimation algorithm is very suitable for real applications and is almost entirely independent of the different levels of modulation techniques used. Also, it has been concluded that the BER perfor-

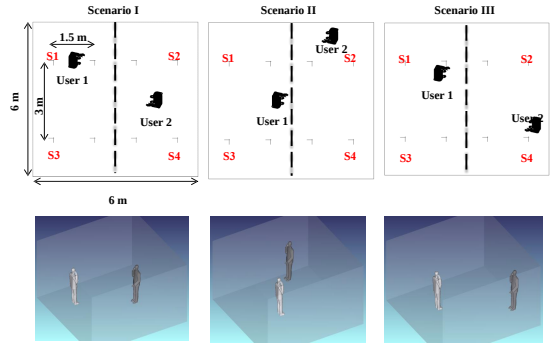

Fig. 4. Locations of Bob and Eve in three different scenarios

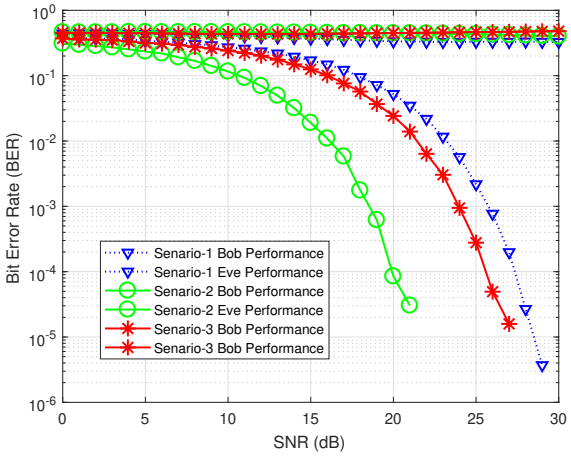

Fig. 5. BER vs. SNR performance of Bob and Eve

mance obtained in the presence of imperfect CSI was very close to that of the BER performance when the channel is known perfectly.

In addition, a novel physical security technique was presented for indoor VLC systems based on GLIM OFDM. In computer simulations, VLC channels for different scenarios are generated by Zemax©, an optical design software with ray-tracing capabilities. Simulation results have shown that as the legitimate user achieved excellent bit error rate (BER) performances, the performance of the eavesdropper degraded to a level that it was impossible to receive any meaningful information.

REFERENCES

[1] Z. Ghassemlooy, L. N. Alves, S. Zvanovec, M. A. Khalighi, Eds., Visible Light Communications: Theory and Applications, CRC press, 2017.

[2] F. Miramirkhani and M. Uysal, "Channel modeling and characterization for visible light communications," IEEE Photon. J., vol. 7, no. 6, Dec. 2015.

[3] Y. Tanaka, T. Komine, S. Haruyama, and M. Nakagawa, "Indoor visible communication utilizing plural white LEDs as lighting," in Proc. 12th IEEE Int. Symp. Pers., Indoor Mobile Radio Commun. (PIMRC), vol. 2. Sep. 2001, pp. F-81–F-85.

[4] J. Armstrong and A. J. Lowery, "Power efficient optical OFDM," Electron. Lett., vol. 42, no. 6, pp. 370–372, Mar. 2006.

[5] M. A. Khalighi, S. Long, S. Bourennane, Z. Ghassemlooy, "PAM- and CAP-Based Transmission Schemes for Visible-Light Communications," in IEEE Access, vol. 5, pp. 27002-27013, 2017, doi: 10.1109/ACCESS.2017.2765181.

[6] N. Fernando, Y. Hong, and E. Viterbo, "Flip-OFDM for optical wireless communications," in Proc. IEEE Inf. Theory Workshop, Paraty, Brazil, Oct. 2011, pp. 5–9.

[7] D. Tsonev and H. Haas, "Avoiding spectral efficiency loss in unipolar OFDM for optical wireless communication," in Proc. IEEE Int. Conf. Commun. (ICC), Sydney, NSW, Australia, Jun. 2014, pp. 3336–3341.

[8] M. S. Islim, D. Tsonev, and H. Haas, "On the superposition modulation for OFDM-based optical wireless communication," in Proc. IEEE Global Conf. Signal Inf. Process. (GlobalSIP), Orlando, FL, USA, Dec. 2015, pp. 1022–1026.

[9] M. W. Eltokhey, M. A. Khalighi, Z. Ghassemlooy, "Multiple Access Techniques for VLC in Large Space Indoor Scenarios: A Comparative Study," 2019 15th International Conference on Telecommunications (ConTEL), Graz, Austria, 2019, pp. 1-6.

[10] Q. Wang, Z. Wang, and L. Dai, "Multiuser MIMO-OFDM for visible light communications," IEEE Photon. J., vol. 7, no. 6, pp. 1–11, Dec. 2015.

[11] R. Mesleh, H. Elgala, and H. Haas, "Optical spatial modulation," IEEE/OSA J. Opt. Commun. Netw., vol. 3, no. 3, pp. 234–244, Mar. 2011.

[12] C. He, T. Q. Wang, and J. Armstrong, "Performance comparison between spatial multiplexing and spatial modulation in indoor MIMO visible light communication systems," in Proc. IEEE Int. Conf. Commun. (ICC), Kuala Lumpur, Malaysia, May 2016, pp. 1–6.

[13] E. Bektas and E. Panayirci, "Channel Estimation for DCO-OFDM Based VLC Systems in the Presence of Clipping Noise", IEEE 28th Signal Processing and Communications Applications Conference (SIU)", 5 - 7 Ekim 2020, Virtual.

[14] E. Bektas and E. Panayirci, "Sparse Channel Estimation with Clipping Noise in DCO-OFDM Based VLC Systems", IEEE International Black Sea Conference on Communications and Networking (BlackSeaCom), 26-29 May 2020, Virtual.

[15] A. Yesilkaya, E. Basar, F. Miramirkhani, E. Panayirci, M. Uysal and H. Haas, "Optical MIMO-OFDM with generalized LED index modulation," IEEE Transactions on Communications, vol. 65, no. 8, pp. 3429-3441, Aug. 2017, doi: 10.1109/TCOMM.2017.2699964.

[16] S. R. Aghdam and T. M. Duman, "Physical layer security for space shift keying transmission with precoding,' IEEE Wireless Commun. Lett., vol. 5, no. 2, pp. 180-183, Apr. 2016.

[17] Y. Chen, L. Wang, Z. Zhao, M. Ma, and B. Jiao, "Secure multiuser MIMO downlink transmission via precoding-aided spatial modulation," IEEE Commun. Lett., vol. 20, no. 6, pp. 1116-1119, Jun. 2016.

[18] F. Wu, R. Zhang, L.-L. Yang, and W. Wang, "Transmitter precoding aided spatial modulation for secrecy communications," IEEE Trans. Veh. Technol., vol. 65, no. 1, pp. 467-471, Jan. 2016.

[19] A. Arafa, E. Panayirci, and V. H. Poor, "Relay-aided secure broadcasting for visible light communications;' IEEE Trans. Commun., vol. 67, no. 6, pp. 4227-4239, Jun. 2019. [67] Z. Huang, Z. Gao, and L. Sun, "An

[20] E. Panayirci, A. Yesilkaya, T. Cogalan, H. Haas, and H. V. Poor, "Physical-layer security with generalized space shift keying," IEEE Trans. Commun., vol. 68, no. 5, pp. 3042-3056, May 2020.

[21] N. Su, E. Panayirci, M. Koca, A. Yesilkaya , H. V. Poor, and H. Haas, "Physical layer security for multi-user MIMO visible light communication systems with generalized space shift keying," IEEE Trans. Commun., vol. 69, no. 4, pp. 2585-2598, Apr. 2021.

[22] E. Panayirci, A. Yesilkaya, T. Cogalan, S. Erkucuk, Y. Sadi, H. Haas and H. V. Poor, "Physical-layer security in visible light communications",IEEE 2nd 6G Summit 2020, 17-20 March 2020, Levi, Finland.

[23] N. Su, E. Panayirci, M. Koca, H. V. Poor, "Spatial Constellation Design Based Generalized Space Shift Keying for Physical Layer Security of Multi-User MIMO Communication Systems", IEEE Wireless Comm. Letters, vol.10, no.8, pp.1785-1789, Aug. 2021.